RSC Advances

PAPER

View Article Online
View Journal | View Issue

Cite this: *RSC Adv.*, 2017, **7**, 21476

Facile fabrication of a magnetic self-healing poly(vinyl alcohol) composite hydrogel

Mingsen Chen, Guisheng Gong, Li Zhou* and Faai Zhang*

Received 23rd December 2016
Accepted 10th April 2017

DOI: 10.1039/c6ra28634h

rsc.li/rsc-advances

This study proposes a simple method to fabricate a magnetic self-healing poly(vinyl alcohol) (ms-PVA) composite hydrogel. The obtained ms-PVA hydrogel was characterized by vibrating sample magnetometery and transmission electron microscopy. The self-healing property was investigated using a rheometer and tensile strength tests. Results showed that the ms-PVA hydrogel exhibited an excellent self-healing property and controllable magnetic intensity by adjusting the Fe_3O_4 particle content. The added Fe_3O_4 particles did not participate in hydrogen bond interactions but did cause the magnetic properties of the hydrogel. The hydrogel showed the best self-healing performance when the amount of Fe_3O_4 particles was 5 wt% (based on ms-PVA). The ms-PVA composite hydrogel presents a new application of the PVA hydrogel given its facile fabrication process and excellent performance.

1. Introduction

Hydrogels are 3D crosslinked polymeric networks that immobilize large quantities of water (20% to up to a thousand times their dry weight) and remain insoluble because of the presence of crosslinking,[1,2] and have been widely applied in a variety of fields, such as biomaterials in wound dressings,[3] implants and soft contact lenses,[4] and microspheres for controlled drug release.[5] However, with the development of functional materials, common hydrogels still cannot meet some specific needs. As a result, functional hydrogels are currently a hot research topic, and a large number of functional hydrogels have been developed,[6–9] such as ternary interpenetrating microvascular networks,[10] metallo-hydrogels,[11] and peptide based hydrogels.[12]

Magnetic hydrogels are a type of promising functional hydrogel with magnetic properties and can be prepared by two main methods:[13,14] one is to blend pre-synthesized magnetic iron oxide nanoparticles (MIONs) with hydrogels in solution and to crosslink the MIONs with the polymer, the other is *in situ* generation of MIONs in the preparation of hydrogels. Magnetic hydrogels have been widely used in biological fields such as magnetic resonance imaging,[15] magnetically targeted hyperthermia,[16] drug delivery,[17,18] and immobilization of proteins,[19] which have intrinsic magnetic property and favorable biocompatibility. However, magnetic hydrogel is easily damaged during its application, which may affect the normal use of related products and lead to a short service life.[20] Therefore, developing a new types of magnetic hydrogels that automatically heal is needed.

The self-healing concept is derived from the self-healing ability of biology. The human skin could self-heal and regenerate after injury. A material that possesses the self-healing properties can significantly prolong service life and save repair cost.[21] However, traditional hydrogel does not possess self-healing properties. Many researchers have reported the preparation of self-healing hydrogels,[22,23] which have widely attracted the interests of scientists in designing the internal structure of hydrogel with reversible covalent bonding systems (Diels Alder chemistry[24] and acylhydrazone bonds[25]) and non-covalent bonds (π–π stacking,[26] hydrogen bond,[27,28] electrostatic interactions,[29,30] and hydrophobic interactions[31,32]). Zhang *et al.*[33] determined that poly(vinyl alcohol) (PVA) hydrogel prepared using the freezing thawing method could self-repair at room temperature without a stimulus or healing agent. The hydrogel exhibited the highest fracture stress reported so far (approximately 200 kPa). Zhang first reported a straightforward method to prepare a novel magnetic hydrogel with healing ability by facilely mixing carboxy-modified Fe_3O_4 nanoparticles in a dynamic hydrogel composed of chitosan and telechelic difunctional poly(ethylene glycol).[20] The results indicated that introducing the self-healing function into magnetic hydrogel was meaningful.

Thus, this study proposes a facile method to prepare magnetic hydrogel with self-healing ability by facilely mixing Fe_3O_4 particles in the self-healing PVA hydrogel. The effects of Fe_3O_4 particle content on the self-healing ability, mechanical and swelling, and magnetic properties of the PVA hydrogels are investigated.

Guangxi Ministry-Province Jointly-Constructed Cultivation Base for State Key Laboratory of Processing for Nonferrous Metal and Featured Materials, College of Material Science and Engineering, Guilin University of Technology, No. 12 Jiangan Road, Guilin 541004, P. R. China. E-mail: zhangfaai@163.com; zhouli@glut.edu.cn; Fax: +86-773-5897772

2. Experimental

2.1 Materials and methods

Poly(vinyl alcohol) (PVA, M_w = 240 kDa), iron(III) chloride hexahydrate ($FeCl_3 \cdot 6H_2O$) powder, iron(II) ferrous sulfate ($FeSO_4 \cdot 7H_2O$) and ammonia solution (25 wt%) were purchased from Aladdin Chemistry Co. All other reagents were analytical grade and used as received without further purification. Deionized water was used throughout the experiments. The crystal structures of Fe_3O_4 were characterized using an X-ray diffractometer (XRD, PANalytical. B.V.) at a scanning range 2θ of 10° to 90° and rad of 0.04°. The tensile strength was tested on a universal testing machine (DCS-5000, Shimadzu) according to ISO 527-2:1993 at a constant crosshead speed of 100 mm min^{-1}. The magnetic moment was recorded at 300 K on an MPMS XL-7 vibrating-sample magnetometer (VSM). The thermal decomposition behavior of the polymers was examined by thermogravimetry with a heating rate of 10 K min^{-1} in nitrogen atmosphere on a model TA Q500 (USA). Rheological date were obtained from an AR1500EX strain-controlled rheometer using a 25 mm parallel plate geometry at 25 °C and analyzed with the rheology advantage data analysis software. Transmission electron microscope (TEM, JEM-2100F from JEOL) with an accelerating voltage of 200 kV was used. The samples were thin-sectioned after drying at room temperature for 3 d.

The swelling ratio (S) of ms-PVA hydrogels was calculated as follows:

$$S = \frac{W_t - W_0}{W_0} \times 100\%$$

where W_0 and W_t are the mass of the dried ms-PVA composite hydrogels before and after immersion in water, respectively.

2.2 Synthesis of magnetic Fe_3O_4 particles

The Fe_3O_4 nanoparticles are prepared as follows: first, 12.5 g (0.04 mol) of $FeSO_4 \cdot 7H_2O$ and 21.7 g (0.08 mol) of $FeCl_3 \cdot 6H_2O$ were dissolved in 50 mL distilled water. Then, ammonia solution (50 mL) was added to the solution with a stirring speed of 1000 rpm under the protection of dry nitrogen at 40 °C to form a homogeneous solution. The color of the solution changed from light brown to black after mixing the solution, which indicated the formation of Fe_3O_4 nanoparticles. This process was maintained for 30 min, and the temperature was increased to 80 °C to crystallize completely for another 60 min. The precipitate Fe_3O_4 particles were washed by repeating cycles of centrifugation and redispersion in distilled water. Washing was performed five times in distilled water. The final products were dried in a vacuum oven at 60 °C for 24 h, and the Fe_3O_4 nanoparticles were finally obtained.

Table 1 Preparation of magnetic self-heal PVA composite hydrogels

Sample	PVA (g)	Fe_3O_4 (g)	H_2O (g)
ms-PVA-1	30	0.75	100
ms-PVA-2	30	1.50	100
ms-PVA-3	30	2.25	100
ms-PVA-4	30	3.00	100

2.3 Synthesis of magnetic self-healing poly(vinyl alcohol) (ms-PVA) composite hydrogels

A series of ms-PVA samples was prepared by adjusting the feed amounts of Fe_3O_4 nanoparticles to investigate the effect of Fe_3O_4 nanoparticle content on the properties of ms-PVA composite gels (see Table 1). In a typical procedure, 30 g PVA was dissolved in 100 mL distilled water at 95 °C with a stirring speed of 25 rpm for 30 min. A certain amount of Fe_3O_4 particles was added, and the solution was stirred for 1 h. Then, the homogeneous solution was into a mold of the desired dimension and cooled at −25 °C for 1 h, followed by thawing at room temperature for 1 h. Finally, the ms-PVA composite hydrogels were obtained. Unless otherwise stated, the hydrogel used in this work was prepared with a PVA concentration of 30 wt% and subjected to one freezing thawing cycle.

3. Results and discussion

3.1 Preparation of Fe_3O_4 particles

The optical microscope image of Fe_3O_4 particles dispersed in water is presented in Fig. 1. Fig. 1 shows that magnetic Fe_3O_4 particles were dispersed uniformly with an average particle size of 1 μm to 5 μm, and a few particles were connected. Fig. 2 shows the XRD pattern of the sample. Six characteristic peaks for Fe_3O_4 (2θ = 30.1, 35.5, 43.3, 53.4, 57.2 and 62.5) were observed, which indicates the successful preparation of the magnetic Fe_3O_4 particles.[34]

3.2 Preparation of ms-PVA composite hydrogels

The synthetic route of the preparation of ms-PVA composite hydrogels illustrated in Scheme 1. First, PVA solution and an appropriate amount of Fe_3O_4 particles were mixed to form a homogeneous solution. Then, the ms-PVA composite hydrogels were fabricated by freezing and thawing the solution. The synthetic protocol was designed based on the following considerations. On one hand, the PVA molecular chain would crosslink each other to form a network structure by intermolecular or intramolecular hydrogen bonding through freezing

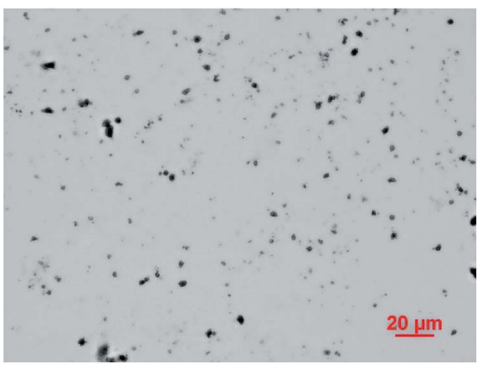

Fig. 1 The optical microscope image of Fe_3O_4 particles.

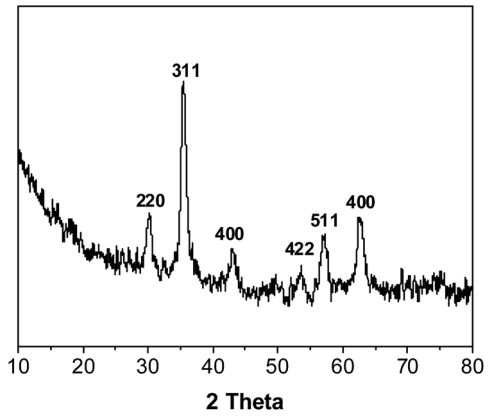

Fig. 2 XRD curve of Fe_3O_4 particles.

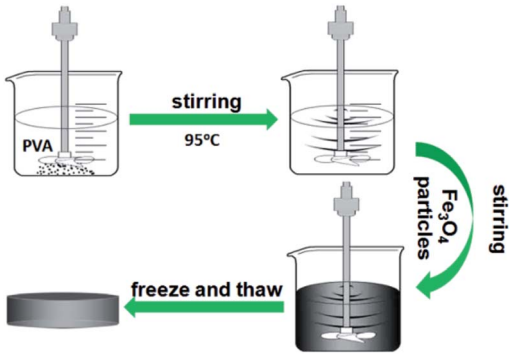

Scheme 1 Synthetic route to the ms-PVA composite hydrogels.

and thawing; the structure consists of crystalline regions and amorphous region.[35] On the other hand, the iron oxide particles could endow PVA with excellent magnetic characteristics and serve as a crosslinker to gelate PVA molecules.[36] Moreover, the hydrogels exhibited excellent self-healing property through the reversible hydrogen bond between the hydroxyl groups because of the existence of a large number of hydroxyl groups in the PVA chain (Fig. 3). Fig. 4 shows the TEM images of ms-PVA hydrogels and ones after prolong freezing time. As shown in Fig. 4, PVA hydrogels all display like dried river beds, for neat PVA, a large

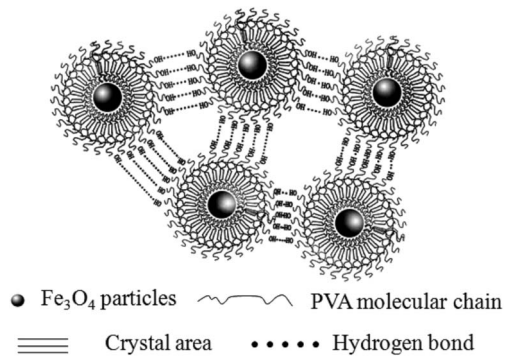

Fig. 3 Internal structure of ms-PVA hydrogels.

number of cracks are observed, which provide relatively good swelling properties of the gel. However, with increasing the feeding amounts of Fe_3O_4 nanoparticles, few cracks are produced, this led to the poor water swelling properties of the hydrogel. In addition, the longer freezing time, the more cracks are formed.

3.3 Thermogravimetric analysis

Thermogravimetric analysis was conducted to investigate the stability of the ms-PVA composite hydrogels further as shown in Fig. 5. Neat PVA hydrogel was almost completely decomposed as the temperature approached 500 °C, and its residue weight was 5.4%. However, the composite gels had lower initial decomposition temperatures and higher final decomposition temperatures and residues compared to neat PVA due to the presence of Fe_3O_4 particles, which resulting in the decrease of the crystallinity of the soft crosslinked gel. The relative differences in the residual weight of composite gels above 500 °C were attributed to the inherently different compositions of Fe_3O_4 particles.

3.4 Magnetic properties

The magnetic properties of Fe_3O_4 particles (Fig. 6a) and the ms-PVA hydrogels (Fig. 6b) were measured by VSM at 300 K. The magnetization curves showed that Fe_3O_4 particles and ms-PVA hydrogels were superparamagnetic with no coercivity at room temperature. The actual saturation magnetization values for Fe_3O_4 particles, ms-PVA-1, ms-PVA-2, ms-PVA-3 and ms-PVA-4 were 64.7, 1.3, 2.7, 4.3 and 5.5 emu g^{-1}, respectively, which were close to the theoretical value (see Table 2). Therefore, the magnetic intensity of the ms-PVA hydrogels can be readily tuned by altering the weight ratio of MIONs. The favorable property of ms-PVA hydrogel promises the remote control property as shown in the inset of Fig. 6b, the circle is the magnet as the external magnetic field, the black is the hydrogel sample, the hydrogel can interact with the magnet under the magnetic effect, so the remote control of the hydrogel can be realized by controlling the shift of the magnet.

3.5 Swelling capacity

The effect of Fe_3O_4 content on the swelling absorption of ms-PVA hydrogels was investigated. Fig. 7 shows that Fe_3O_4 content is an important factor that influences the water absorbency of the composite hydrogels. The increasing Fe_3O_4 weight ratio from 0.0% to 0.1% caused a decrease in water absorbency because of two factors. First, the interaction of the PVA chains with the Fe_3O_4 particles may form some low-mobility regions that can act as additional physical crosslinking points, which reduced the swelling ability of the matrix.[36] Second, the addition of Fe_3O_4 particles reduces the content of PVA in hydrogel, which is the main factor influencing the water-absorbing capacity. Therefore, water absorbency decreased with the increase of in Fe_3O_4 weight ratio.

3.6 Rheological analysis

3.6.1 Fe_3O_4 particle content. The rheological properties of ms-PVA hydrogels were evaluated by dynamic mechanical

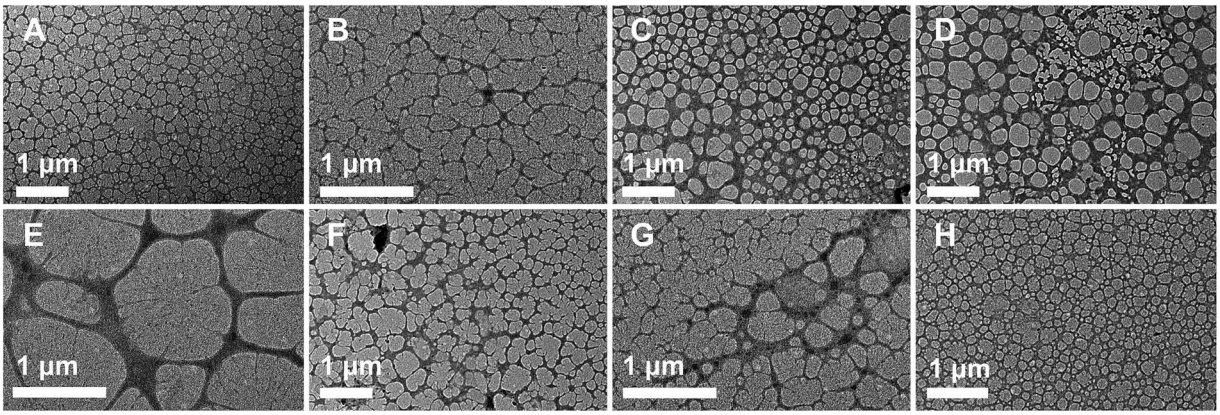

Fig. 4 TEM images of ms-PVA hydrogels and ones after prolong freezing time ((A) neat PVA, (B) ms-PVA-1, (C) ms-PVA-2, (D) ms-PVA-3, (E) ms-PVA-4, (F) ms-PVA-2 freezing time 2 h, (G) ms-PVA-2 freezing time 3 h, (H) ms-PVA-2 freezing time 4 h).

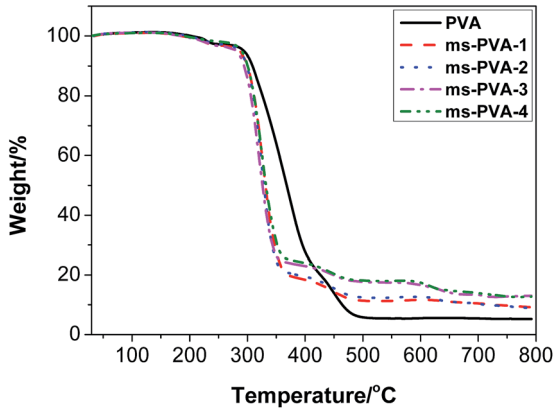

Fig. 5 TGA curve of the hydrogels.

characterization. A series of hydrogels with different ratios of Fe_3O_4 particles was prepared, and the storage modulus G' values *versus* frequency were tested (Fig. 8).

Fig. 8 shows that the value of storage modulus G' is higher than that of loss modulus G'', indicating hydrogel formation.[37] Moreover, with the increase in frequency (0.1 Hz to 100 Hz, strain (%) = 5) particles, the storage modulus G' of the hydrogels increased. The polymer chains could not recover from previous movement in high frequency, indicating the formation of the stable structure of the hydrogels, which was not broken down by the mechanical shear force. Furthermore, a higher G' value was observed for the samples with a high ratio of Fe_3O_4 particles, indicating that the addition of Fe_3O_4 particles had a positive effect on the gelation of PVA aqueous solution.

3.6.2 Freezing time. A series of ms-PVA-2 hydrogels with different freezing times was prepared, and the storage modulus G' values *versus* frequency were tested (Fig. 9). The elastic modulus of the three hydrogels, shows that the storage modulus G' gradually increased with the increase in freezing time, indicating that the internal hydrogel increasingly cross-linked and the hydrogel strength gradually increased, which reduced the PVA molecular mobility.

3.6.3 Number of freezing and thaw cycles. A series of ms-PVA-2 hydrogels with different numbers of freezing and thaw cycles was prepared, and the storage modulus G' values *versus* frequency were tested (Fig. 10). A higher G' value was observed for the samples with more freezing and thaw cycles. This finding could be attributed to the presence of high crystallinity and the degree of crosslinking, which contribute to the strength of the network as the number of freezing and thawing cycles increased. However, the free hydroxyl of the PVA molecule will decrease as the degree of crosslinking increases, which may be unfavourable for the self-healing capacity of the hydrogels.

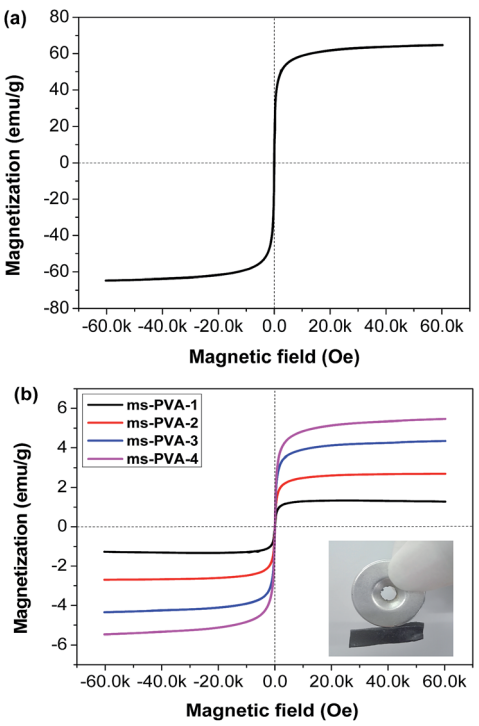

Fig. 6 Magnetic hysteresis loops of Fe_3O_4 particles (a) and the ms-PVA hydrogels (b) at 300 K.

Table 2 Saturation magnetization for Fe_3O_4 particles and the ms-PVA hydrogels

	Fe_3O_4	ms-PVA-1	ms-PVA-2	ms-PVA-3	ms-PVA-4
Saturation magnetization (emu g^{-1})	64.7	1.3	2.7	4.3	5.5
Fe_3O_4 content (%, theoretical)	100	2.4	4.8	7.0	9.1
Fe_3O_4 content (%, actual)	100	2.0	4.2	6.6	8.5

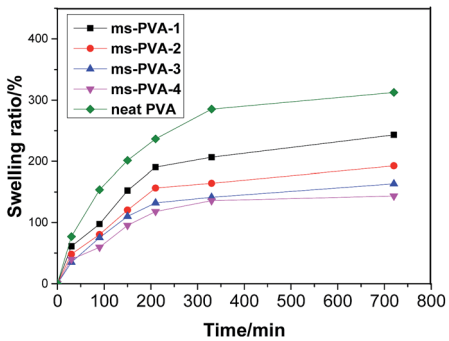

Fig. 7 Swelling ratio of hydrogels.

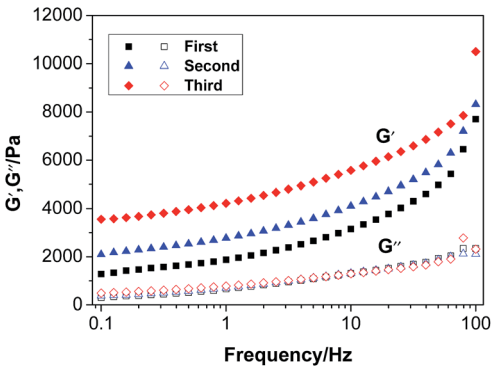

Fig. 10 Frequency scanning of magnetic hydrogels.

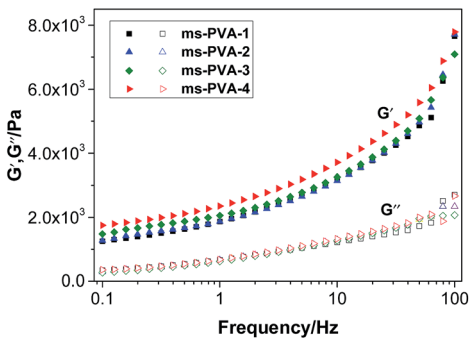

Fig. 8 Frequency scanning of magnetic hydrogels.

3.6.4 Self-healing hydrogel. Rheological analyses were conducted to measure the self-healing process of the ms-PVA-2 hydrogel. After cutting the hydrogel into 8 pieces, the G' and G'' values of self-healing hydrogel *versus* frequency were almost the same as those of the original hydrogel (Fig. 11a), which qualitatively indicate the recovery of the inner structure of the hydrogel. Fig. 11b shows the hydrogel under a pulse deformation program. The strain initially increases from 5% to 200% at a certain time point and then returns to 5% after a certain period. The G' and G'' values are inverted under 1000% strain, which indicates the collapse of the gel network. G' and G'' return to their original values when placed under 5% strain. This recovery behavior could be repeatable for at least four cycles of

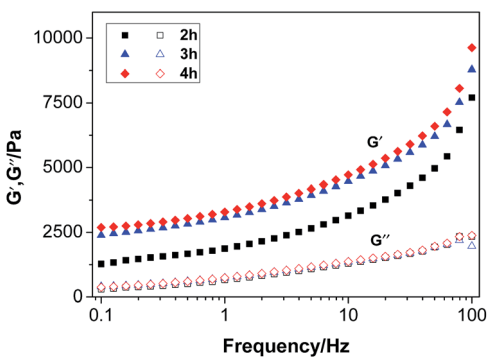

Fig. 9 Frequency scanning of magnetic hydrogels.

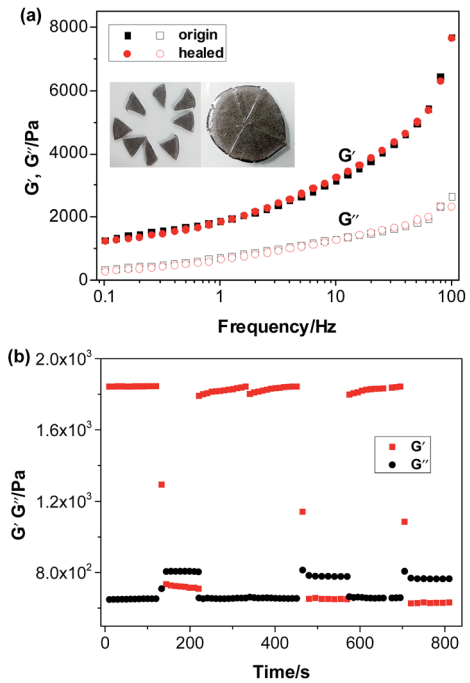

Fig. 11 Frequency (a), strain (b) scanning of hydrogels.

varying strains, which indicates the rapid recovery of the inner network.[38] All results support the self-healing ability of the dynamic hydrogels.

3.7 Self-healing performance

Fe_3O_4 particles in the hydrogel do not affect the dynamic linkage because the hydrogel network is constructed through a reversible hydrogen bond. Thus, the magnetic hydrogel is self-healable, which is proven by the phenomenon shown in Fig. 12. A piece of the original hydrogels (1) was divided into two pieces using scissors (2) and placed together immediately to insure contact of the freshly created fracture surfaces (3). After 12 h, the self-healing hydrogel was stretched to break with a universal testing machine (4). The hydrogel do not even fracture at the wound (5). Thus, the ms-PVA hydrogels have excellent self-healing performance.

3.8 Mechanical properties

3.8.1 Effect of freezing time. Previous studies have shown that the freezing time has an important influence on the self-healing properties of PVA hydrogel. Investigating the effect of freezing time (*i.e.*, 2, 3 and 4 h) on the self-healing properties of ms-PVA-2 hydrogel is important. Fig. 13 shows that, with the increase in freezing time, the tensile strength of the hydrogel significantly increased from 0.2 MPa to 0.78 MPa, whereas the self-healing efficiency decreased from 100% to 9%. The longer the freezing time is, the higher the crosslinking degree of the hydrogel becomes, which leads to the improvement of the tensile strength of the hydrogel.[39] However, less free hydroxyl groups in hydrogel were used for self-healing, which caused the decrease in self-healing efficiency.

3.8.2 Effect of Fe_3O_4 particle content. A series of hydrogels with different Fe_3O_4 particle contents was prepared and the effect of Fe_3O_4 contents on the tensile strength and self-healing efficiency of the hydrogel was investigated. Fig. 14 illustrates

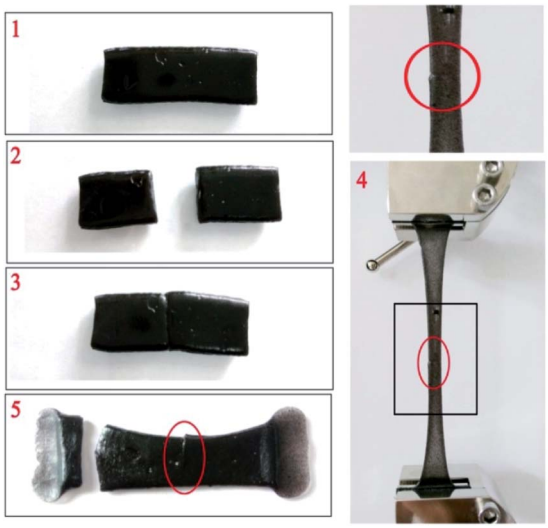

Fig. 12 Self-healing process of magnetic hydrogel ((1) original sample; (2) cutting off; (3) healing; (4) stretching; (5) fracture).

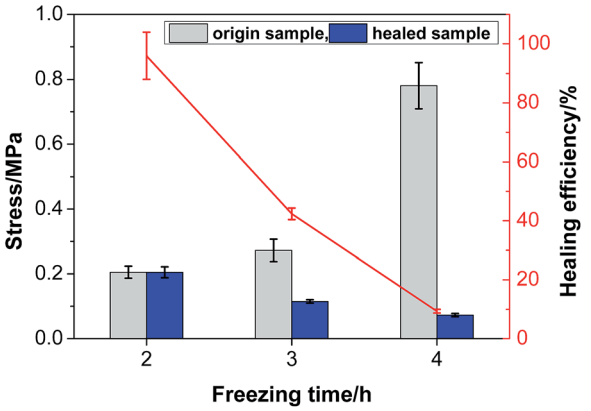

Fig. 13 Effect of freeze time on self-healing properties of ms-PVA-2 hydrogel.

that the tensile strength of the original samples was enhanced from 0.13 MPa to 0.32 MPa as the content of Fe_3O_4 particles increased from 2.5% to 10%. This observation indicated that the Fe_3O_4 particles in the PVA solution exhibited a nucleation effect to promote gel gelation, which results in the improvement of the initial strength of the hydrogel. When the content of Fe_3O_4 particles increased from 2.5% to 5%, the tensile strength after self-healing reached its maximum, and continuously increasing content of Fe_3O_4 particles diminished the self-healing efficiency. The Fe_3O_4 particles exerted an inhibiting effect on the binding of free hydroxyl groups through hydrogen bond when the content of Fe_3O_4 particles was more than 5%. Therefore, the ms-PVA-2 hydrogel exhibited the best self-healing strength and self-healing efficiency when the content of Fe_3O_4 particles was 5%.

3.8.3 Effect of the number of freezing and thawing. The effects of the number of freezing and thawing cycles on the self-healing properties of the ms-PVA-2 hydrogel were investigated. Fig. 15 shows that the self-healing efficiency of the hydrogels decreases drastically as the number of freezing and thawing cycles increases. The PVA hydrogel prepared using the freezing and thawing method became harder and more opaque with the

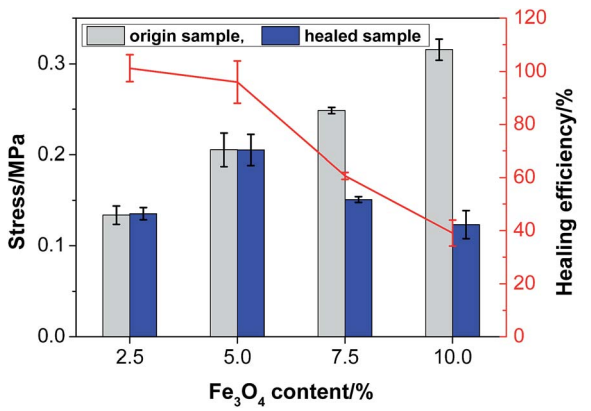

Fig. 14 Effect of Fe_3O_4 content of self-healing properties of ms-PVA hydrogels.

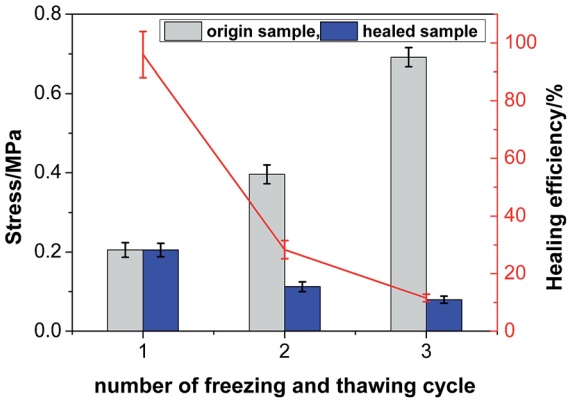

Fig. 15 Effect of freezing and thawing times on self-healing properties of ms-PVA-2 hydrogel.

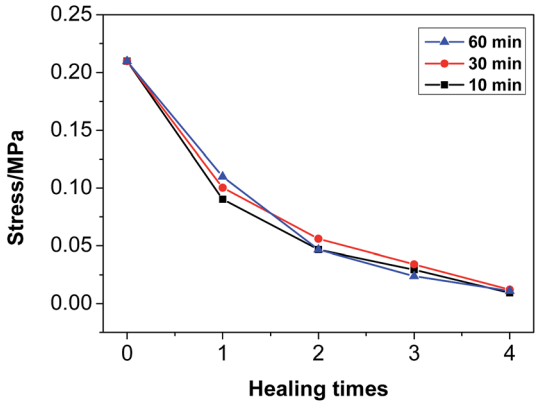

Fig. 17 Repeat self-healing properties of ms-PVA-2 hydrogel.

increase in the number of freezing thawing cycles as a result of the increased crystallinity of PVA chains.[40] Generally, greater hardness of the hydrogel means lesser chain mobility, which indicates that the molecular chains on the two surfaces cannot migrate or diffuse from one side to the other. Thus the self-healing process cannot develop effectively. This finding explains the decrease in the fracture stress of self-healing hydrogel with the increase in the number of freezing and thawing cycles.

3.8.4 Healing time. The effect of healing time on the self-healing efficiency was evaluated because healing time is a crucial parameter for practical application. Fig. 16 shows that the self-healing efficiency increased rapidly in the initial stage within the first 60 min slowly increased and reached 100% after 12 h. The rapid step of self-healing efficiency in the beginning was due to the existence of a large number of free OH^- on the fracture surface and excellent chain mobility.[33] These results indicated the occurrence of a rapid and efficient autonomous self-healing process in such physically crosslinked ms-PVA hydrogel.

3.8.5 Repeat self-healing properties. For self-healing materials, the repeat self-healing performance is important to the service life of the material. Fig. 17 shows the repeat self-healing performance of the ms-PVA-2 hydrogel. Repair times were set at 10, 30, and 60 min. The figure shows that the tensile strength after healing is high for the first healing in all three conditions. Healing efficiency reached 42%, 48% and 54%, respectively. The longer the repair time is, the higher the healing efficiency becomes. This finding can be attributed to increased uncrosslinked hydroxyl groups on the fractured hydrogel surface and improved molecular mobility. Afterward, the healing efficiency was reduced for later freezing and thawing cycles. The hydrogels lose their self-healing ability when they were repaired for the fourth time, they lose self-healing ability because of the decrease in the molecular mobility of the fracture surface. Therefore, PVA-124 hydrogels exhibited relatively good repeated self-healing performance.

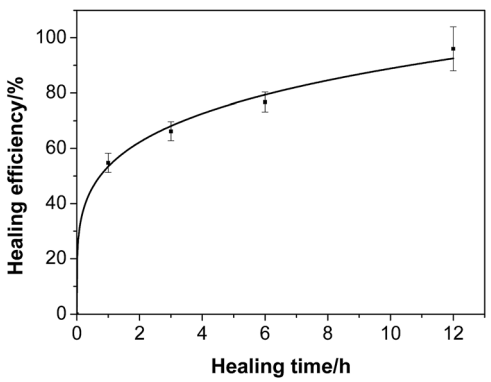

Fig. 16 Effect of healing time on self-healing properties of ms-PVA-2 hydrogel.

4. Conclusions

In summary, this study proposed an easy and viable strategy to fabricate superparamagnetic self-healing bifunctional PVA composite hydrogels by simply adding magnetic iron oxide particles to physically crosslinked PVA hydrogel by freezing and thawing. The obtained ms-PVA hydrogels show a controllable magnetic property by adjusting the magnetic iron oxide content. Moreover, the addition of magnetic iron oxide particles largely affects the self-healing property of the ms-PVA hydrogel because of its influence on the crosslinked structure of the composite hydrogel. The results highlight the combined advantages of self-healing and magnetic hydrogels, which extend the application of the PVA hydrogel.

Acknowledgements

The authors greatly acknowledgement the financial support from the Natural Science Foundation of China (21364003, 51263004).

References

1 J. Jagur-Grodzinski, *Polym. Adv. Technol.*, 2010, **21**, 27–47.

2 M. Ahmad, S. M. Rai and A. Mahmood, *Adv. Polym. Technol.*, 2016, **35**, 121–128.
3 H.-J. Gwon, Y.-M. Lim, S.-J. An, M.-H. Youn, S.-H. Han, H.-N. Chang and Y.-C. Nho, *Korean J. Chem. Eng.*, 2009, **26**, 1686–1688.
4 B. S. Fazly Bazzaz, B. Khameneh, M.-m. Jalili-Behabadi, B. Malaekeh-Nikouei and S. A. Mohajeri, *Cont. Lens Anterior Eye*, 2014, **37**, 149–152.
5 M. Montiel-Herrera, A. Gandini, F. M. Goycoolea, N. E. Jacobsen, J. Lizardi-Mendoza, M. Recillas-Mota and W. M. Argüelles-Monal, *Carbohydr. Polym.*, 2015, **128**, 220–227.
6 M. Liu, Y. Ishida, Y. Ebina, T. Sasaki, T. Hikima, M. Takata and T. Aida, *Nature*, 2015, **517**, 68–72.
7 F. Song, X. Li, Q. Wang, L. Liao and C. Zhang, *J. Biomed. Nanotechnol.*, 2015, **11**, 40–52.
8 Y. J. Che, D. P. Li, Y. L. Liu, Q. L. Ma, Y. B. Tan, Q. Y. Yue and F. J. Meng, *RSC Adv.*, 2016, **6**, 106035–106045.
9 M. Criado, J. M. Rey, C. Mijangos and R. Hernandez, *RSC Adv.*, 2016, **6**, 105821–105826.
10 C. J. Hansen, S. R. White, N. R. Sottos and J. A. Lewis, *Adv. Funct. Mater.*, 2011, **21**, 4320.
11 S. Basak, J. Nanda and A. Banerjee, *Chem. Commun.*, 2014, **50**, 2356–2359.
12 K. Basu, A. Baral, S. Basak, A. Dehsorkhi, J. Nanda, D. Bhunia, S. Ghosh, V. Castelletto, I. W. Hamley and A. Banerjee, *Chem. Commun.*, 2016, **52**, 5045–5048.
13 L. Zhou, B. He and F. Zhang, *ACS Appl. Mater. Interfaces*, 2011, **4**, 192–199.
14 G. Gong, F. Zhang, Z. Cheng and L. Zhou, *Int. J. Biol. Macromol.*, 2015, **81**, 205–211.
15 A. Fernández-Ferreiro, M. González Barcia, M. Gil-Martínez, A. Vieites-Prado, I. Lema, B. Argibay, J. Blanco Méndez, M. J. Lamas and F. J. Otero-Espinar, *Eur. J. Pharm. Biopharm.*, 2015, **94**, 342–351.
16 M. Häring, J. Schiller, J. Mayr, S. Grijalvo, R. Eritja and D. D. Díaz, *Gels*, 2015, **1**, 135–161.
17 G. R. Mahdavinia, H. Etemadi and F. Soleymani, *Carbohydr. Polym.*, 2015, **128**, 112–121.
18 N. Zhang, J. Lock, A. Sallee and H. Liu, *ACS Appl. Mater. Interfaces*, 2015, **7**, 20987–20998.
19 F.-Y. Chou, C.-M. Shih, M.-C. Tsai, W.-Y. Chiu and S. J. Lue, *Polymer*, 2012, **53**, 2839–2846.
20 Y. Zhang, B. Yang, X. Zhang, L. Xu, L. Tao, S. Li and Y. Wei, *Chem. Commun.*, 2012, **48**, 9305–9307.
21 S. R. White, N. Sottos, P. Geubelle, J. Moore, M. R. Kessler, S. Sriram, E. Brown and S. Viswanathan, *Nature*, 2001, **409**, 794–797.
22 D. L. Taylor and M. In Het Panhuis, *Adv. Mater.*, 2016, **28**, 9060–9093.
23 Y. Zhang, B. Yang, L. Xu, X. Zhang, L. Tao and Y. Wei, *Acta Phys.-Chim. Sin.*, 2013, **71**, 485–492.
24 Z. Wei, J. H. Yang, X. J. Du, F. Xu, M. Zrinyi, Y. Osada, F. Li and Y. M. Chen, *Macromol. Rapid Commun.*, 2013, **34**, 1464–1470.
25 G. Deng, F. Li, H. Yu, F. Liu, C. Liu, W. Sun, H. Jiang and Y. Chen, *ACS Macro Lett.*, 2012, **1**, 275–279.
26 Y. Xu, Q. Wu, Y. Sun, H. Bai and G. Shi, *ACS Nano*, 2010, **4**, 7358–7362.
27 A. Phadke, C. Zhang, B. Arman, C.-C. Hsu, R. A. Mashelkar, A. K. Lele, M. J. Tauber, G. Arya and S. Varghese, *Proc. Natl. Acad. Sci. U. S. A.*, 2012, **109**, 4383–4388.
28 M. M. C. Bastings, S. Koudstaal, R. E. Kieltyka, Y. Nakano, A. C. H. Pape, D. A. M. Feyen, F. J. van Slochteren, P. A. Doevendans, J. P. G. Sluijter, E. W. Meijer, S. A. J. Chamuleau and P. Y. W. Dankers, *Adv. Healthcare Mater.*, 2014, **3**, 70–78.
29 X. Wang, F. Liu, X. Zheng and J. Sun, *Angew. Chem., Int. Ed.*, 2011, **50**, 11378–11381.
30 Q. Wang, J. L. Mynar, M. Yoshida, E. Lee, M. Lee, K. Okuro, K. Kinbara and T. Aida, *Nature*, 2010, **463**, 339–343.
31 U. Gulyuz and O. Okay, *Soft Matter*, 2013, **9**, 10287–10293.
32 G. Jiang, C. Liu, X. Liu, G. Zhang, M. Yang, Q. Chen and F. Liu, *J. Macromol. Sci., Part A: Pure Appl. Chem.*, 2010, **47**, 335–342.
33 H. Zhang, H. Xia and Y. Zhao, *ACS Macro Lett.*, 2012, **1**, 1233–1236.
34 Y. Zhou, T. Fan, R. Yang, H. Sun and Q. Xia, *J. Pharm. Sci.*, 2007, **16**, 187.
35 H. Hong, H. Liao, S. Chen and H. Zhang, *Mater. Lett.*, 2014, **122**, 227–229.
36 J. S. Gonzalez, C. E. Hoppe, D. Muraca, F. H. Sanchez and V. A. Alvarez, *Colloid Polym. Sci.*, 2011, **289**, 1839–1846.
37 S. Li, H.-Y. Lu, Y. Shen and C.-F. Chen, *Macromol. Chem. Phys.*, 2013, **214**, 1596–1601.
38 P. Sahoo, R. Sankolli, H.-Y. Lee, S. R. Raghavan and P. Dastidar, *Chem.–Eur. J.*, 2012, **18**, 8057–8063.
39 N. A. Peppas and S. R. Stauffer, *J. Controlled Release*, 1991, **16**, 305–310.
40 M. Lee, H. Bae, S. Lee, N.-o. Chung, H. Lee, S. Choi, S. Hwang and J. Lee, *Macromol. Res.*, 2011, **19**, 130–136.